ARTICLES

^{51}V ESE-ENDOR Studies of Oxovanadium(IV) Complexes: Investigation of the Nuclear Quadrupole Interaction

Christopher V. Grant,† James A. Ball,† Brent J. Hamstra,‡ Vincent L. Pecoraro,‡ and R. David Britt*,†

Department of Chemistry, University of California, Davis, California 95616, and Department of Chemistry, University of Michigan, Ann Arbor, Michigan 48109

Received: January 28, 1998; In Final Form: July 29, 1998

The technique of ^{51}V electron spin echo−electron nuclear double resonance (ESE-ENDOR) has been used to investigate a structurally diverse series of oxovanadium(IV) complexes. From ENDOR spectra, ^{51}V nuclear quadrupole coupling constants, which reflect the electric field gradient established at the vanadium nucleus, are estimated using a perturbation theory approach. The magnitude of the nuclear quadrupole interaction is reduced by ligands binding trans to the oxygen of the oxovandium moiety due to a reduction of the electric field gradient that is established primarily by the oxo bond. Variation of ligands containing nitrogen and oxygen donor atoms oriented cis to the oxo bond gives rise to minimal changes in the quadrupole coupling constant. The nuclear quadrupole coupling constant is thus shown to be sensitive to ligands binding trans to the oxygen of the oxo bond. ENDOR can thusly serve as a new spectroscopic probe in the identification of weakly coordinating donors in the axial position such as may be found in vanadyl-substituted proteins.

Introduction

The use of vanadyl, the oxovanadium(IV) (VO^{2+}) ion, in EPR studies of metal ion binding sites within systems of biological interest has been well established.[1] Structural information in such systems is derived from electron g and ^{51}V hyperfine matrix components. In particular, the application of the additivity relationship, which utilizes trends in the magnitude of hyperfine components, has been found useful for defining the number and types of ligands bound cis to the oxo group in the equatorial plane.[2] CW EPR studies are insensitive to ligation in the axial position trans to the oxo moiety of the complex ion.[2] However, these weakly associated axial ligands may contribute to the formation of vanadyl binding sites in proteins.

The techniques of electron nuclear double resonance (ENDOR) and electron spin echo envelope modulation (ESEEM) have been used to obtain quadrupolar and hyperfine matrix components of ligands involved in VO^{2+} binding.[1] For example, these techniques have been useful in the identification of equatorial amine and imidazole nitrogen donors.[3−7] However, only recently have axial amine nitrogen donors been identified via ESEEM.[8] Typically, these axial ligands cannot be reliably identified by measuring VO^{2+} g and hyperfine matrixes alone.[2]

The large anisotropy of the vanadyl hyperfine matrix and the presence of the $I = {}^{7}/_{2}$ ^{51}V quadrupole moment have led us to investigate the high frequency orientation-selected ENDOR of the following vanadyl complexes. Of particular interest is the possibility that the measurement of the quadrupolar tensor components will assist in the identification of axial ligands found at the apical site trans to the oxo bond. 2,3,7,8,12,13,17,18-Octaethylporphinatooxovanadium(IV) (VO(oep)), displayed in Figure 1a, is a well-characterized molecule that has been studied structurally by EPR methods and X-ray crystallography and which allows for well-defined axial ligand binding since the rigid coordination geometry of VO(oep) does not allow for structural isomers.[9−12] Vanadyl porphyrins are of general interest, as they are found as a contaminant in crude oils, typically in the form of vanadyl etioporphyrin, for which VO(oep) is a synthetic model.[13] Additionally, the well-characterized vanadyl complexes, bis(acetylacetonato)oxovanadium(IV) ($VO(acac)_2$) displayed in Figure 1b, and the oxovanadium(IV) derivative of *N*,*N*′-ethylenebis(salicylideneamine) (VO(salen)) displayed in Figure 1c, have been investigated. Structural studies of $VO(acac)_2$ adducts via EPR and X-ray crystallography as well as by infrared spectroscopy have been reported.[14−17] Previous studies of $VO(acac)_2$ have provided evidence for sixth ligand binding cis to the vanadyl oxygen for ligands such as pyridine. Figure 1b illustrates the structural isomers. VO(salen) has been studied structurally by EPR, ENDOR, and X-ray crystallography.[18,19]

Magnetic Resonance Background and Theory

The highly anisotropic vanadyl spin system (electron spin $S = {}^{1}/_{2}$, nuclear spin $I = {}^{7}/_{2}$) allows for single-crystal-like ENDOR spectra to be obtained at the $M_I = \pm{}^{7}/_{2}$ parallel turning points of the EPR spectrum.[20] The spin Hamiltonian is constructed as follows, with electron Zeeman, hyperfine, isotropic nuclear Zeeman, and electric nuclear quadrupole terms, respectively:

* Corresponding author.
† University of California.
‡ University of Michigan.

S1089-5647(98)00912-2 CCC: $15.00
Published on Web 09/09/1998

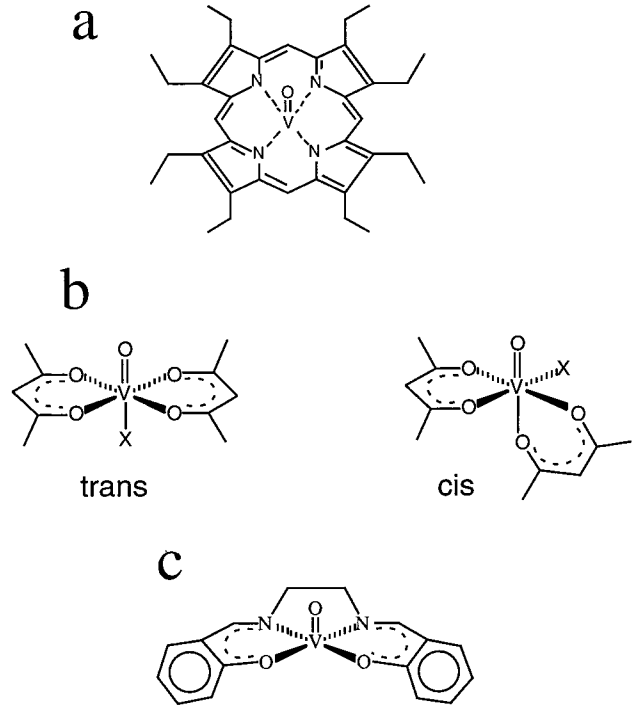

Figure 1. Structures of (a) VO(oep) and (b) cis and trans additional ligand binding configurations of $VO(acac)_2$ adducts, where X represents the additional ligand, and (c) VO(salen).

$$H = \beta\vec{B}\cdot\mathbf{g}\cdot\vec{S} + \vec{S}\cdot\mathbf{A}\cdot\vec{I} - \beta_n g_n\vec{B}\cdot\vec{I} + \vec{I}\cdot\mathbf{P}\cdot\vec{I} \qquad (1)$$

Figure 2 displays a "single-crystal" energy level diagram for the vanadyl spin system constructed with the above spin Hamiltonian. In its principal axis system, the traceless nuclear quadrupole tensor **P** can be represented by the parameters $P_{||}$ and η, where $P_{||} = (3/2)P_{zz} = 3e^2qQ/[4I(2I-1)]$ (specifically $3e^2qQ/84$ for $I = {}^7/_2$) and $\eta = |(P_{xx} - P_{yy})|/P_{zz}$,[21] where q is the electric field gradient along the principal axis of the largest field gradient, and Q is the ^{51}V nuclear quadrupole moment (-0.05×10^{-24} cm^2).[22] The nuclear quadrupole coupling constant (nqcc) $P_{||}$ therefore specifies the field gradient along the z axis. The asymmetry parameter η is a measure of gradient asymmetry in the plane perpendicular to the z axis and may range from zero for the special case of axial symmetry to one in the fully rhombic limit. The nuclear quadrupole interaction term of the Hamiltonian, $\vec{I}\cdot\mathbf{P}\cdot\vec{I}$ in the principal axis system can be rewritten as

$$P_{||}[\{I_z^2 - (1/3)I(I+1)\} + (\eta/3)\{I_x^2 - I_y^2\}] \qquad (2)$$

The matrix form of the quadrupole interaction within its principal axis system is

$$\mathbf{P} = P_{||}/3\begin{pmatrix} -(1-\eta) & 0 & 0 \\ 0 & -(1+\eta) & 0 \\ 0 & 0 & 2 \end{pmatrix} \qquad (3)$$

Perturbation theory can be used to derive useful analytical expressions for the ^{51}V ENDOR frequencies. In the following expressions, the pure nuclear terms in the Hamiltonian are taken to first order, and the ^{51}V hyperfine interaction is extended to second order. Analytical expressions can be derived for the ENDOR frequencies of the two ENDOR transitions (a and d or b and c, Figure 2) ($\nu^{||}$), obtained at the parallel turning point of a specific M_I EPR transition powder pattern, as well as the average frequency of the two ENDOR transitions ($\tilde{\nu}^{||}$) and their difference ($\Delta\nu^{||}$). These expressions are particularly simple in the case where all interactions are assumed axial with a collinear z axis (the VO bond axis). With these assumptions, the following expressions apply to $\Delta M_I = +1$ ENDOR transitions:

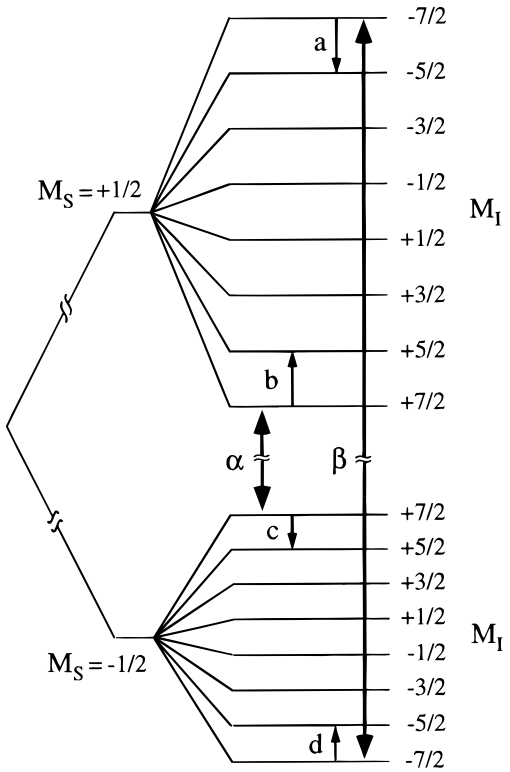

Figure 2. Energy level diagram obtained from the spin Hamiltonian (equation 1), where β represents the EPR transition for $M_I = -{}^7/_2$ where a and d represent the associated ENDOR transitions. The EPR transition for $M_I = +{}^7/_2$ is represented by α, where b and c represent the associated ENDOR transitions.

$$\nu^{||} = A_{||}/2 + A_\perp{}^2(2M_I+1)/4\nu_0 \pm A_\perp{}^2/4\nu_0 \pm g_n\beta_n B \mp P_{||}(2M_I+1) \qquad (4)$$

$$\Delta\nu^{||} = A_\perp{}^2/2\nu_0 + 2g_n\beta_n B - 2P_{||}(2M_I+1) \qquad (5)$$

$$\tilde{\nu}^{||} = A_{||}/2 + A_\perp{}^2(2M_I+1)/4\nu_0 \qquad (6)$$

We then define $\Delta\Delta\nu^{||}_{\pm}(7/2)$ as the difference in the $\Delta\nu^{||}$ splittings obtained at the $M_I = +{}^7/_2$ and $-{}^7/_2$ parallel turning points.

$$\Delta\nu^{||}(+{}^7/_2) - \Delta\nu^{||}(-{}^7/_2) = \Delta\Delta\nu^{||}_{\pm}(7/2) = 2g_n\beta_n(B_{+7/2} - B_{-7/2}) - 24P_{||} \qquad (7)$$

The nqcc parameter is then calculated using this analytical perturbation theory result.

Experimental Section

EPR. The pulsed EPR/ENDOR spectrometer has been previously described.[23,24] All experiments were carried out at X-band microwave frequencies. Spectra were recorded at temperatures between 10 and 15 K utilizing the Davies ENDOR sequence ($\pi - T - \pi/2 - \tau - \pi - \tau -$ echo with the rf pulse applied during the time T).[25] Field swept electron spin echo (ESE) EPR spectra were recorded utilizing the two-pulse echo sequence ($\pi/2 - \tau - \pi - \tau -$ echo) with the echo intensity

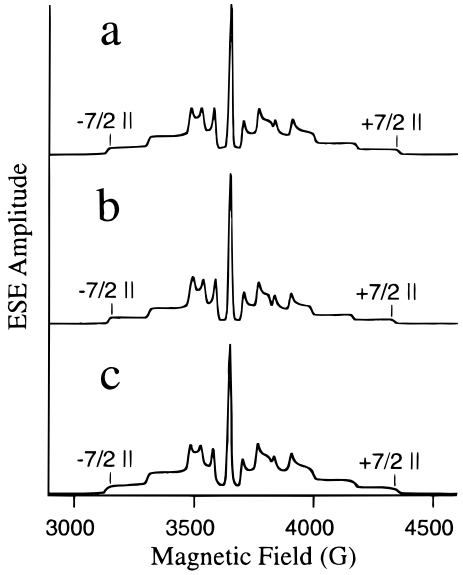

Figure 3. ESE-EPR magnetic field sweeps of VO(oep) adducts for (a) no axial ligand, (b) *n*-butylamine, and (c) imidazole. ENDOR field positions are labeled. Spectra were taken at a temperature of 14 K, in toluene. Experimental conditions were as follows: $\nu_{mw} = 10.275$ GHz; $\tau = 350$ ns; $\pi/2$ MW pulse duration = 40 ns; π MW pulse duration 80 ns; MW power ~ 3.5 W for (a) and ~3.2 W for (b) and (c).

monitored as a function of magnetic field. Relatively long microwave pulses (40−120 ns) were used to allow the best possible orientation selection for the Davies ENDOR experiment.[26] ENDOR rf pulses were 18 μs in duration for VO(salen) and VO(acac) complexes and 20 μs in duration for VO(oep) complexes, with a power of 100 W and a frequency increment of 0.2 MHz. In all cases the time T was 2 μs greater than the rf pulse duration. ENDOR field positions were selected such that ESE intensity is monitored at the top edge of the parallel $M_I = \pm^7/_2$ turning points of the ESE-detected EPR spectrum (Figure 3). All ENDOR spectra were fit to Gaussian curves for the determination of the splittings, as in Figure 4. The error in perturbation theory estimates of $P_{||}$ is determined by the statistical error of the Gaussian fits. All values of $P_{||}$ are reported to ±0.003 MHz for VO(acac) and VO(salen) complexes and to ±0.01 MHz for VO(oep) complexes, with the larger errors for the VO(oep) complexes because for these compounds the ENDOR transitions overlap when observed at the parallel turning point of the $M_I = -^7/_2$ EPR transition. The sign of $P_{||}$ is determined to be the same as the hyperfine interaction, which in this work is assumed negative.[27] Preliminary matrix diagonalization calculations show that these perturbation theory calculations of $P_{||}$ do not provide perfect numerical values, but the trends over a ligand series can be usefully analyzed in this simple approach. For more accurate absolute magnitudes of $P_{||}$ and for analysis of asymmetry parameters (which we cannot yet confidently estimate with perturbation theory), we are developing a systematic matrix diagonalization analysis. This will also allow for the study of nonaxially symmetric systems as well as the possible affects of axis rotations in future work.

Samples. The VO(oep) and VO(acac)$_2$ compounds were purchased from Aldrich and used without further purification. All solvents were dried and distilled. Samples of VO(oep) were prepared at 3.5 mM concentration in toluene. This concentration was chosen to minimize intermolecular interactions. All VO(acac)$_2$ samples were prepared at 5 mM concentration in a solvent system of 1:1 by volume of toluene and methylene chloride. In all cases additional ligands are present in a 1−2-fold molar excess. VO(salen) was prepared by the method of Pasquali et al. and recrystallized from acetonitrile prior to use.[28] VO(salen) was prepared at 5 mM concentration in a solvent system of 1:1 by volume of toluene and methylene chloride.

Results and Discussion

VO(oep). The rigid structure of VO(oep) allows for addition of axial ligands while coordination in the plane of the complex is essentially unchanged. The vanadium ion of VO(oep) without an additional axial ligand is displaced 0.543 Å above the plane of the four coordinating nitrogens of the porphyrin in the direction of the oxygen atom of the oxo bond.[11] The value of the nqcc, $P_{||}$, is determined by the electric field gradient q established primarily by the strong oxo bond. Addition of an axial ligand acts to diminish the field gradient along this principal axis. Because of the nonplanar geometry of the VO(oep) complex, steric considerations bias the selection of axial ligands. The axial ligands chosen for this experiment are *n*-butylamine and imidazole. Investigations of axial ligand binding for vanadyl porphyrins are reported in the literature, and for these ligands, binding constants have been reported for the similar vanadyl tetraphenylporphyrin.[29] ESE-detected EPR field sweeps are shown in Figure 3, and the field positions where ENDOR was performed are indicated. The ENDOR spectra of Figure 4 illustrate how the difference in the splitting of

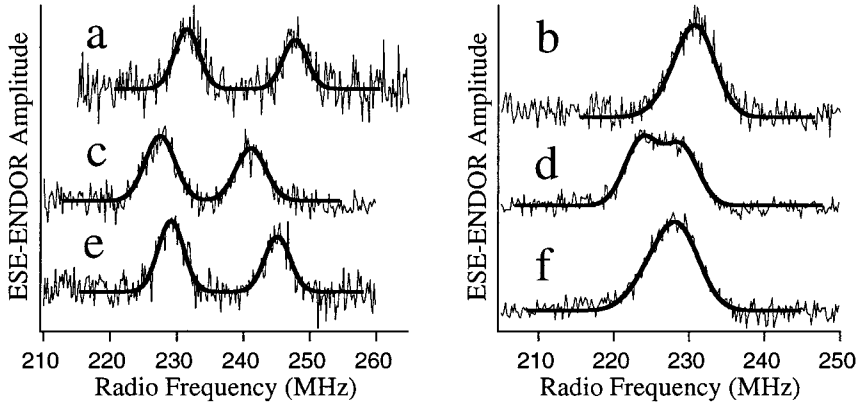

Figure 4. ENDOR spectra for VO(oep) at (a) the $+^7/_2||$ EPR transition (4345 G) and (b) the $-^7/_2||$ EPR transition (3145 G); VO(oep) coordinated axially by *n*-butylamine at (c) the $+^7/_2||$ EPR transition (4324 G) and (d) the $-^7/_2||$ EPR transition (3152 G); VO(oep) coordinated axially by imidazole at (e) the $+^7/_2||$ EPR transition (4336 G) and (f) the $-^7/_2||$ EPR transition (3150 G). The field positions are indicated in Figure 3. The Gaussian fits are shown as smooth curves. Experimental conditions were as follows: $\nu_{mw} = 10.275$ GHz; $\tau = 350$ ns; $\pi/2$ MW pulse duration = 40 ns; π MW pulse duration = 80 ns; MW power ~ 3.5 W for (a) and (b) and ~3.2 W for (c−f); ENDOR rf pulse duration = 20 μs; $T = 22$ μs; rf power ~ 100 W.

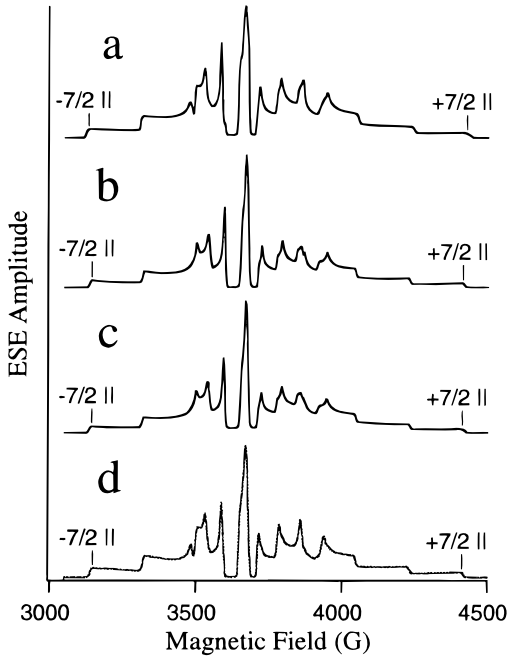

Figure 5. ESE-EPR magnetic field sweeps for $VO(acac)_2$ with (a) no additional ligand (b) DMSO (c) ethanol and (d) pyridine. Spectra were taken at a temperature of 15 K in a solvent of 1:1 by volume of toluene and methylene chloride. Field positions for ENDOR experiments are indicated. Experimental conditions were as follows: $\nu_{mw} = 10.297$ GHz; $\tau = 550$ ns; $\pi/2$ MW pulse duration = 120 ns; π MW pulse duration = 240 ns; MW power $\sim$ 0.28 W.

ENDOR transitions at the $\pm^7/_2$ parallel EPR transitions is sensitive to the coordination environment of the ion (and the associated quadrupolar coupling constant). Figure 4a,b displays ENDOR spectra for VO(oep) in toluene glass. With the axial binding site vacant, VO(oep) gives rise to a pair of ENDOR transitions separated by 16.24 MHz obtained at the $M_I = +^7/_2$ parallel turning point, with this splitting estimated by Gaussian fits to the observed transitions. The splitting of the transitions at the $M_I = -^7/_2$ parallel turning point is estimated at 3.30 MHz when the observed spectral features are fit to a pair of Gaussian curves. This leads to a calculated quadrupolar coupling constant of -0.43 MHz using eq 7. The z component of the electric field gradient is predominantly established by the strong oxo bond. ENDOR spectra for VO(oep) coordinated axially by *n*-butylamine are shown in Figure 4c,d. When the vacant axial site is coordinated by *n*-butylamine, $P_{||}$ is calculated from the ENDOR spectra to be -0.24 MHz, a significant reduction in magnitude from the case in which the axial site is vacant, indicative of a diminution of the electric field gradient at the ^{51}V nucleus. The ENDOR spectra for VO(oep) coordinated axially by imidazole are displayed in Figure 4e,f. $P_{||}$ is calculated to be -0.40 MHz, indicating that the imidazole ligand

TABLE 1: Summary of Estimated Values for $\Delta\nu^{||}(+^7/_2||)$, $\Delta\nu^{||}(-^7/_2||)$, $\Delta\Delta\nu^{||}_{-}(^7/_2)$, $P_{||}$[a]

complex	$\Delta\nu(+^7/_2)$ (MHz)	$\Delta\nu(-^7/_2)$ (MHz)	$\Delta\Delta\nu$ (MHz)	$P_{||}$ (MHz)
VO(oep)	16.24	3.30	12.94	−0.43
VO(oep) + *n*-butylamine	13.61	5.28	8.33	−0.24
VO(oep) + imidazole	15.96	3.79	12.17	−0.40
VO(acac)	16.53	3.33	13.20	−0.429
VO(acac) + DMSO	13.89	5.66	8.23	−0.224
VO(acac) + ethanol	14.24	5.39	8.85	−0.250
VO(acac) + pyridine	12.50	7.03	5.47	−0.110
VO(salen)	16.12	3.02	13.10	−0.431
VO(salen) + pyridine	15.10	3.60	11.50	−0.369

[a] All of these values are reported in MHz. All values of $P_{||}$ for $VO(acac)_2$ and VO(salen) are reported to ± 0.003 MHz and ± 0.01 MHz for VO(oep) complexes.

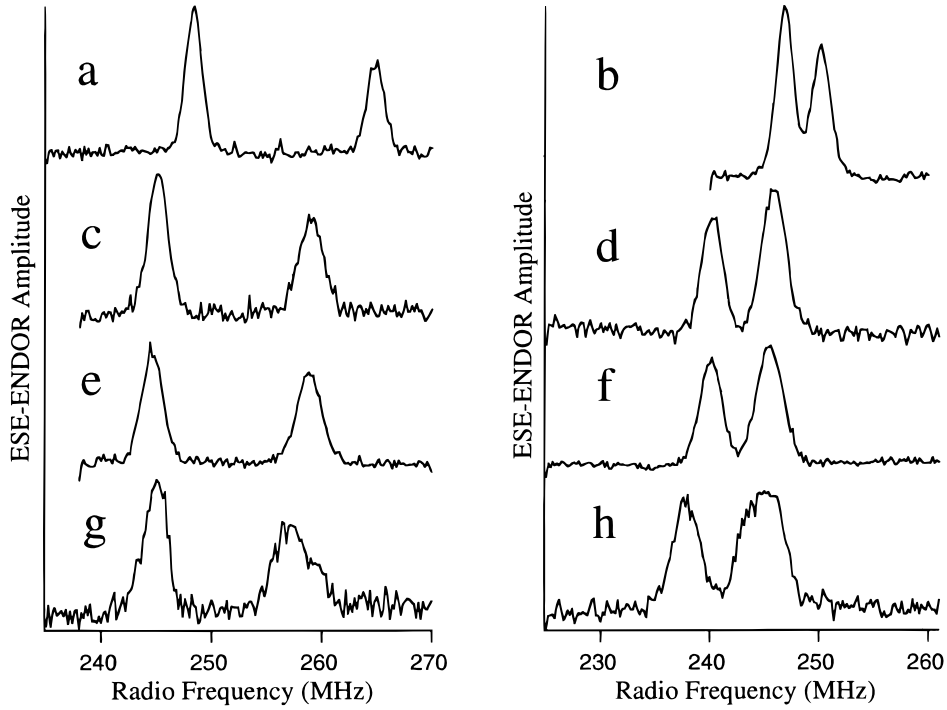

Figure 6. ESE-ENDOR of $VO(acac)_2$ taken at (a) the $+^7/_2||$ EPR transition (4426 G) and (b) the $-^7/_2||$ EPR transition (3128 G); $VO(acac)_2$ with additional ligand DMSO at (c) the $+^7/_2||$ EPR transition (4414 G) and (d) the $-^7/_2||$ EPR transition (3142 G); $VO(acac)_2$ with additional ligand ethanol at (e) the $+^7/_2||$ EPR transition (4412 G) and (f) the $-^7/_2||$ EPR transition (3142 G); $VO(acac)_2$ with additional ligand pyridine at (g) the $+^7/_2||$ EPR transition (4412 G) and (h) the $-^7/_2||$ EPR transition (3146 G). Experimental conditions were as follows: $\nu_{mw} = 10.297$ GHz; $\tau = 550$ ns; $\pi/2$ MW pulse duration = 120 ns; π MW pulse duration = 240 ns; MW power $\sim$ 0.28 W; ENDOR rf pulse duration = 18 μs; $T = 20$ μs; rf power $\sim$ 100 W.

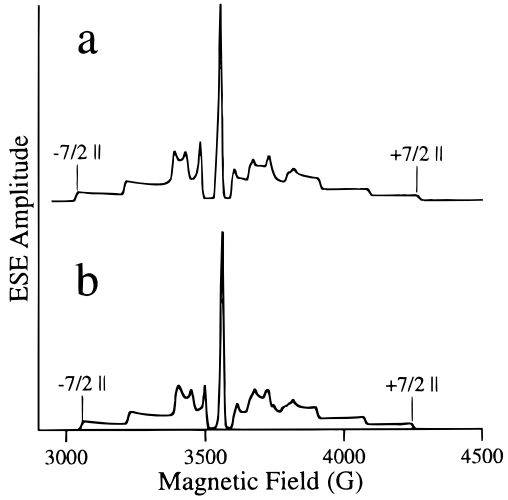

Figure 7. ESE-EPR magnetic field sweep of (a) VO(salen) and (b) VO(salen) with additional pyridine ligand. ENDOR field positions are indicated. Experimental conditions were as follows: $\nu_{mw} = 9.999$ GHz; $\tau = 450$ ns; $\pi/2$ MW pulse duration = 100 ns; π MW pulse duration = 200 ns; MW power ~ 0.50 W.

is less effective than *n*-butylamine in diminishing the electric field gradient established by the oxo bond. These data are summarized in Table 1. The $\pm^7/_2$ parallel turning points are significantly less sharp in the field sweep for VO(oep) coordinated axially by imidazole (Figure 3c). This is possibly due to a significant presence of VO(oep) with a vacant axial binding site as a species in solution, or perhaps a hyperfine "strain" that is the result of different binding orientations of the imidazole ligand, resulting in slightly differing magnetic resonance properties for molecules of a given orientation. This is further evidenced by the unusual line shape of the ENDOR spectra, which could be the result of two sets of overlying ENDOR transitions from two distinct species.

VO(acac)$_2$. The VO(acac)$_2$ complex and the resulting adducts formed by addition of ethanol, DMSO, and pyridine have been investigated. Figure 5 displays ESE magnetic field sweeps for these complexes. It is noted that solution structures of VO(acac)$_2$ adducts have been studied by ligand ENDOR.[14] In the case of no additional ligand or in the presence of weakly binding ligands, the predominant structure has been proposed to consist of equatorial binding of the acetylacetonato groups. It has also been concluded that, for the case of the strong binding ligand pyridine, the resulting adduct structure shows evidence of pyridine binding predominantly cis to the oxo bond rather than at the axial site, as illustrated in Figure 1b. The nqcc measured in this work are consistent with the proposed structures. ENDOR spectra for the studied VO(acac)$_2$ adducts are shown in Figure 6. In the case of unbound VO(acac)$_2$, $P_{||}$ is calculated from the ENDOR splittings to be -0.429 MHz, and with the bound axial ligands of ethanol and DMSO $P_{||}$ is calculated to be -0.250 and -0.224 MHz, respectively. The calculated nqcc for the pyridine adduct is -0.110 MHz. This number indicates very strong binding at the axial site, which would be expected of the structure proposed by Kirste and van Willigen,[14] in which the pyridine binds cis to the oxo group and one of the acetylacetonato ligands is displaced, allowing for an oxygen of the acetylacetonato group to bind from the trans position while the other binds cis to the oxo bond. The *cis*-pyridine adduct of VO(acac)$_2$ is also the structure proposed by LoBrutto et al.[8] upon reexamination of earlier literature reports of ESEEM and ENDOR results.[14,30] Although an equilibrium between the cis and trans isomers is not obvious in the EPR spectrum, ENDOR line shapes for the pyridine adduct are slightly distorted, which may indicate a significant presence of the isomer in which pyridine binds axially, as concluded by IR studies.[16,17] These data are consistent with those obtained in the study of VO(oep). The measured $P_{||}$ approaches zero as the electric field gradient established by the oxo bond is diminished by the addition of axial ligands. In the case of bound ethanol and DMSO, $P_{||}$ differs from the unbound case by only a small amount, indicating a small contribution of electron density along the *z* axis opposite the oxo group. In the case of acetylacetonate binding in the axial position, much more electron density is donated along the *z* axis, resulting in a smaller electric field gradient and a diminished magnitude of $P_{||}$.

VO(salen). The VO(salen) complex allows for comparison of quadrupole coupling constants for the case where the vanadyl ion is coordinated by both oxygen donor atoms and nitrogen donor atoms in the plane cis to the oxo bond. Figure 7 displays ESE-detected EPR magnetic field sweeps for VO(salen) and VO(salen) coordinated axially by pyridine, and Figure 8 displays ENDOR data for these complexes. The nqcc $P_{||}$ is calculated to be -0.431 MHz for VO(salen). The formation of the pyridine adduct gives rise to a nqcc of -0.369 MHz. The relative change in the magnitude of $P_{||}$ upon addition of an axial pyridine ligand is small when compared to changes exhibited by axial ethanol and DMSO coordination of VO(acac)$_2$. This could possibly be due to the distorted square-pyramidal geometry of VO(salen)

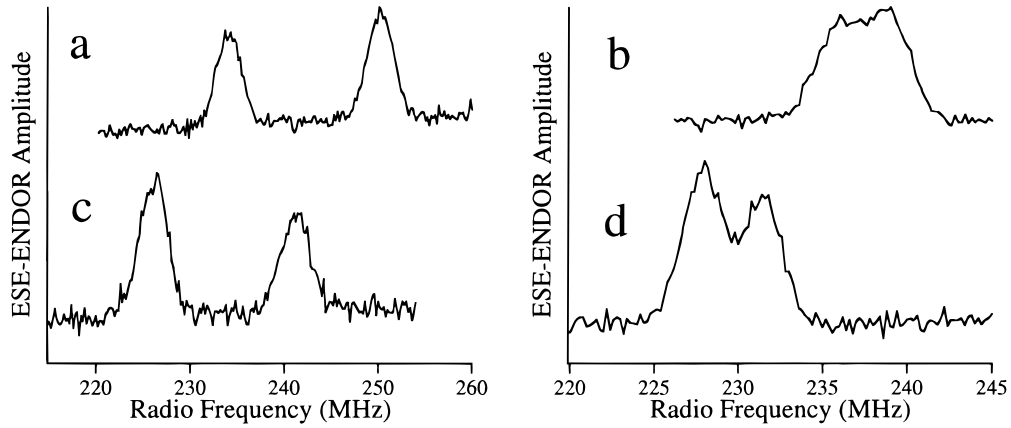

Figure 8. ENDOR spectra of VO(salen) at (a) the $+^7/_2||$ EPR transition (4262 G) and (b) the $-^7/_2||$ EPR transition (3034 G); VO(salen) with additional pyridine ligand at (c) the $+^7/_2||$ EPR transition (4240 G) and (d) the $-^7/_2||$ EPR transition (3054 G). Experimental conditions were as follows: $\nu_{mw} = 9.999$ GHz; $\tau = 450$ ns; $\pi/2$ MW pulse duration = 100 ns; π MW pulse duration = 200 ns; MW power ~ 0.50 W; ENDOR rf pulse duration = 18 μs; $T = 20$ μs; rf power ~ 100 W.

sterically hindering ligand binding.[19] Table 1 compares the measured values of $P_{||}$, and serves to illustrate the similarity of the magnitude of $P_{||}$ for VO(oep), $VO(acac)_2$, and VO(salen) all with vacant axial binding positions. The electric field gradient along the principal axis established by the oxo bond seems to be influenced very little by the different coordination environments in the plane cis to the oxo bond.

Conclusion

High-frequency ^{51}V ENDOR has been used to investigate the nuclear electric quadrupole interaction, which is on the order of 1000 times smaller in energy than the hyperfine interaction and is therefore not readily available from the EPR spectrum alone. The ENDOR technique, however, allows for the sensitive measure of the ^{51}V nuclear quadrupole coupling constant. The ^{51}V ENDOR experiment reveals information about the coordination environment of the vanadyl ion. Our work demonstrates that the coordination of vanadyl complexes at the axial site greatly influences the electric field gradient established by the oxo bond of vanadyl and that the nature of the nonaxial ligands has little influence on the electric field gradient along the principal axis and thus little influence on the magnitude of the nqcc, $P_{||}$. Bound axial ligands contribute electron density from the axial position, the result of which is a diminished electric field gradient at the vanadium nucleus and a nqcc that is smaller in magnitude.

Such measurements may be useful for identifying the types and locations of ligands in complexes of unknown coordination, particularly in biological systems. Several X-ray structures of V(V)-substituted proteins that contain axially bound ligands have appeared.[31−33] Two recent studies suggest that the axially bound ligands are also likely contributors to the coordination environments of VO^{2+}-substituted proteins. The presence of an axially coordinated lysine in VO^{2+}-substituted chloroplast F_1-ATPase has been proposed on the basis of ESEEM measurements of this system,[34] and a recent EPR and ESEEM study of model complexes suggests that an axially coordinated histidine ligand may be bound to vanadium in the reduced, inactive form of the vanadium-dependent haloperoxidases.[8,35] The data reported here indicate that ENDOR should be able to serve as an additional spectroscopic probe of these and similar systems, providing independent information about coordination spheres in biologically relevant environments.

Acknowledgment. This work was supported by grants from the NIH (GM42703 to V.L.P. and GM48242 to R.D.B.). In this special edition of *The Journal of Physical Chemistry B*, we thank Melvin Klein and Kenneth Sauer for all the inspiration they have given us over the years. Their contributions in pioneering and applying new spectroscopic methods to the study of complex biological systems have been extraordinary.

References and Notes

(1) Eaton, S. S.; Eaton, G. R. In *Vanadium in Biological Systems*; Chasteen, N. D., Ed.; Kluwer Academic Publishers: Boston, 1990; pp 199−222.

(2) Chasteen, N. D. In *Biological Magnetic Resonance*; Berliner, L. J.; Reuben, J., Eds.; Plenum Press: New York, 1981; pp 53−119.

(3) Mulks, C. F.; Kirste, B.; van Willigen, H. *J. Am. Chem. Soc.* **1982**, *104*, 5906.

(4) Tipton, P. A.; McCracken, J.; Cornelius, J. B.; Peisach, J. *Biochemistry* **1989**, *28*, 5720.

(5) Hanna, P. M.; Chasteen, N. D.; Rottman, G. A.; Aisen, P. *Biochemistry* **1991**, *30*, 9210.

(6) Zhang, C.; Markham, G. D.; LoBrutto, R. *Biochemistry* **1993**, *32*, 9866.

(7) Dikanov, S. A.; Tyryshkin, A. M.; Hittermann, J.; Bogumil, R.; Witzel, H. *J. Am. Chem. Soc.* **1995**, *117*, 4976.

(8) LoBrutto, R.; Hamstra, B. J.; Colpas, G. J.; Pecoraro, V. L.; Frasch, W. D. *J. Am. Chem. Soc.* **1998**, *120*, 4410.

(9) Fukui, K.; Ohya-Nishiguchi, H.; Kamada, H. *J. Phys. Chem.* **1993**, *97*, 11858.

(10) Bonnett, R.; Brewer, P.; Noro, K.; Noro, T. *Tetrahedron* **1978**, *34*, 379.

(11) Molinaro, F. S.; Ibers, J. A. *Inorg. Chem.* **1976**, *13*, 2278.

(12) Mulks, C. F.; van Willigen, H. *J. Phys. Chem.* **1981**, *85*, 1220.

(13) Triebs, A. *Angew. Chem.* **1936**, *49*, 682.

(14) Kirste, B.; van Willigen, H. *J. Phys. Chem.* **1982**, *86*, 2743.

(15) Dodge, R. P.; Templeton, D. H.; Zalkin, A. J. *J. Chem. Phys.* **1961**, *35*, 55.

(16) Caire, C. M.; Haigh, J. M.; Nassimbeni, L. R. *J. Inorg. Nucl. Chem. Lett.* **1972**, *8*, 109.

(17) Caire, C. M.; Haigh, J. M.; Nassimbeni, L. R. *J. Inorg. Nucl. Chem.* **1972**, *34*, 3171.

(18) Attanasio, D. *J. Phys. Chem.* **1986**, *90*, 4952.

(19) Riley, P. E.; Pecoraro, V. L.; Carrano, C. J.; Bonadies, J. A.; Raymond, K. N. *Inorg. Chem.* **1986**, *25*, 154.

(20) van Willigen, H. *J. Magn. Reson.* **1980**, *39*, 37.

(21) Abragam, A.; Bleaney, B. *Electron Paramagnetic Resonance of Transition Ions*; Dover Publications: New York, 1986; pp 166−167.

(22) Weltner, W., Jr. *Magnetic Atoms and Molecules*; Dover: New York, 1983; p 342.

(23) Sturgeon, B. E.; Britt, R. D. *Rev. Sci. Instrum.* **1992**, *63*, 2187.

(24) Sturgeon, B. E.; Ball, J. A.; Randall, D. W.; Britt, R. D. *J. Phys. Chem.* **1994**, *98*, 12871.

(25) Davies, E. R. *Phys. Lett.* **1974**, *47A*, 1.

(26) Hoffman, B. M.; DeRose, V. J.; Doan, P. E.; Gurbiel, R. J.; Houseman, A. L. P.; Telser, J. In *Biological Magnetic Resonance*; Berliner, I. J., Reuben, J., Eds.; Plenum: New York, 1993; Vol. 13, pp 151−218.

(27) Strach, S. J.; Bramley, R. *Chem. Phys. Lett.* **1984**, *109*, 363.

(28) Pasquali, M.; Marchetti, F.; Floriani, C.; Merlino, S. *J. Chem. Soc., Dalton Trans.* **1977**, 139.

(29) Bencosme, C. S.; Romero, C.; Simoni, S. *Inorg. Chem.* **1985**, *24*, 1603.

(30) Astashkin, A. V.; Dikanov, S. A.; Tsvetkov, Yu. D. *J. Struct. Chem.* **1985**, *26*, 363.

(31) Lindqvist, Y.; Schneider, G.; Vihko, P. *Eur. J. Biochem.* **1994**, *221*, 139.

(32) Messerschmidt, A.; Wever, R. *Proc. Natl. Acad. Sci. U.S.A.* **1996**, *93*, 392.

(33) Zhang, M.; Zhou, M.; Van Etten, R. L.; Stauffacher, C. V. *Biochemistry* **1997**, *36*, 15.

(34) Houseman, A. L. P.; LoBrutto, R.; Frasch, W. D. *Biochemistry* **1995**, *34*, 3277.

(35) Hamstra, B. J.; Houseman, A. L. P.; Colpas, G. J.; Kampf, J. W.; LoBrutto, R.; Frasch, W. D.; Pecoraro, V. L. *Inorg. Chem.* **1997**, *36*, 4866.